

Doping dependence of an *n*-type cuprate superconductor investigated by ARPES

N.P. Armitage^a, F. Ronning^b, D.H. Lu, C. Kim^c, A. Damascelli, K.M. Shen, D.L. Feng^d, H. Eisaki, and Z.-X. Shen
Dept. of Physics, Applied Physics and Stanford Synchrotron Radiation Laboratory, Stanford University, Stanford, CA 94305

P.K. Mang, N. Kaneko, and M. Greven

Dept. of Applied Physics and Stanford Synchrotron Radiation Laboratory, Stanford University, Stanford, CA 94305

Y. Onose, Y. Taguchi, and Y. Tokura

Department of Applied Physics, The University of Tokyo, Tokyo 113-8656, Japan

(November 20, 2001)

We present an angle resolved photoemission (ARPES) doping dependent study of the *n*-type cuprate superconductor $\text{Nd}_{2-x}\text{Ce}_x\text{CuO}_{4\pm\delta}$, from the half-filled Mott-insulator to the $T_c=24\text{K}$ superconductor. In Nd_2CuO_4 , we reveal for the first time the charge transfer band (CTB). As electrons are doped to the system, spectral weight forms near- E_F with a concomitant decrease in the intensity of this CTB. At low doping, the Fermi surface is an electron-pocket (with volume $\sim x$) centered at $(\pi,0)$. Further doping leads to the creation of a new LDA-like Fermi surface (volume $\sim 1+x$) that stems from the connection of the $(\pi,0)$ states and from states that were at higher energy near $(\pi/2,\pi/2)$ moving to E_F . These findings shed light on the Mott gap, its doping dependence, as well as the anomalous transport properties of the *n*-type cuprates.

PACS numbers: 79.60.Bm, 73.20.Dx, 74.72.-h

The parent compounds of the high-temperature superconductors are believed to belong to a class of materials known as Mott insulators [1]. At half-filling (one charge carrier per unit cell) these materials, predicted to be metallic by band theory, are insulating due to the large on-site Coulomb repulsion that inhibits double site occupation and hence charge conduction. These cuprates become metals and then superconductors when doped with charge carriers away from half-filling. Although the general systematics of Mott insulators and metals are understood, the question of how one may proceed from a half-filled Mott insulator with only low-energy spin degrees of freedom to a metal with a large Luttinger theorem respecting Fermi surface is unresolved. Even after 15 years of intensive research into this fundamental issue in the cuprates, both the manner in which this evolution occurs and the nature of electronic states at the chemical potential is unclear.

Within the Hubbard model, Mott insulators are described as a single metallic band that is split into an upper Hubbard band (UHB) and a lower Hubbard band (LHB) by a correlation energy U that represents the energy cost for a site to be doubly occupied. The high- T_c parent compounds are not Mott insulators *per se*, but may be more properly characterized as charge transfer insulators [2]. It is believed that such systems can be described by an effective Hubbard Hamiltonian, where an oxygen-derived charge transfer band (CTB) that is energetically split off from the main valence band (due to strong Cu-O hybridization) substitutes for the LHB and the charge transfer gap Δ plays the role of U . At half-filling the LHB (UHB) is totally occupied (unoccupied)

with the chemical potential inside the insulator's gap. Photoemission measurements on the prototypical half-filled parent Mott insulators $\text{Sr}_2\text{CuO}_2\text{Cl}_2$ (SCOC) and $\text{Ca}_2\text{CuO}_2\text{Cl}_2$ (CCOC) have shed light on the dispersive behavior of the CTB [3,4]. Interestingly, previous photoemission measurements on undoped Nd_2CuO_4 (NCO) did not reveal a similar feature [5]. This is surprising as one might expect that the half-filled CuO_2 planes would exhibit generalities independent of material class.

In the simplest picture, the chemical potential shifts into the LHB or UHB (with a transfer of spectral weight across the correlation gap $\sim U$ [6]), as the material is doped away from half-filling with holes or electrons respectively. In alternative scenarios, the act of doping creates "states" inside the insulator's gap, and as a result the chemical potential remains fixed in the middle of the gap [7,8]. A definitive resolution to this issue has been hampered by the lack of reliable inverse photoemission experiments, that in principle, coupled with photoemission could show where the E_F states reside with respect to the CTB and UHB. Information culled from photoemission alone on different materials been interpreted in terms of both scenarios [7–9].

The vast majority of photoemission experiments on the high-temperature superconductors have been performed on hole-doped materials [10,11]. In contrast, the electron-doped materials have been relatively unexplored [7,12–14]. In addition to having interesting properties of their own, the electron-doped materials provide a unique opportunity to explore the evolution from a Mott insulator to a metal as a greater portion of the states is occupied, making a full view of the Mott gap possible for

photoemission experiments.

In this Letter, we report results of an angle resolved photoemission spectroscopic (ARPES) study of the electron-doped cuprate superconductor $\text{Nd}_{2-x}\text{Ce}_x\text{CuO}_{4\pm\delta}$ at concentrations $x = 0, 0.04, 0.10$, and 0.15 . For the first time, we are able to isolate and resolve the contribution to the spectra from the CTB on the $x = 0$ sample as has been observed in the parent compounds of the hole-doped materials thereby demonstrating the universality of the electronic structure of the CuO_2 plane. In NCCO this feature appears ~ 1.3 eV below the Fermi energy, making almost the entire Mott gap visible in our experiment. Upon doping, spectral weight is shifted from the CTB to form states near E_F . At very low doping, these states are centered around $(\pi, 0)$, forming a small Fermi surface with volume $\sim x$. Simultaneously, there is an appearance of spectral weight that begins to span and fill the insulator's gap. At high doping levels, this in-gap spectral weight moves to E_F near $(\pi/2, \pi/2)$ and thereby connects with $(\pi, 0)$ derived states to form an LDA-like Fermi surface with volume $\sim 1 + x$. For $x = 0.15$, it is only states at the intersection between the Fermi surface (FS) and the antiferromagnetic Brillouin zone boundary that retain their unusual properties. This evolution provides a natural explanation for the confusing transport data from electron-doped materials, and is qualitatively similar to what one expects from some $t - t' - t'' - U$ models.

Single crystals of $\text{Nd}_{2-x}\text{Ce}_x\text{CuO}_{4\pm\delta}$ (NCCO) with concentrations $x = 0, 0.04, 0.10$, and 0.15 were grown by the traveling-solvent floating-zone method in 4 atm. of O_2 at Stanford University ($x = 0.04, 0.10$, and 0.15) and the University of Tokyo ($x = 0$ and 0.15). Samples of $x = 0.10$ and 0.15 were oxygen reduced. In addition some data were taken on reduced $x = 0.04$ samples and were found to have features intermediate between unreduced $x = 0.04$ and reduced $x = 0.10$. Measurements were performed at the Stanford Synchrotron Radiation Laboratory's Beamline 5-4. The data reported here were collected with 16.5 eV photons with 10-20 meV energy resolution and an angular resolution as good as 0.25° ($\sim 1\%$ of the Brillouin zone) except where indicated. The chamber pressure was lower than 4×10^{-11} torr. In all measurements sample temperatures were uniformly 10-20K. This presented no charging problems even for the $x = 0$ insulator. Cleaving the samples *in situ* at 10K resulted in shiny flat surfaces, which LEED revealed to be clean and well ordered with the same symmetry as the bulk [13,14]. No signs of surface aging were seen for the duration of the experiments (~ 24 h).

In Figs. 1(a) and 1(b) we show the results of a comprehensive momentum space survey of the undoped NCO system with polarization of the incoming photons at 45° to the Cu-O bonds. Along the Γ to (π, π) cut, a large broad feature disperses out from under the main valence band, reaches a maximum near $(\pi/2, \pi/2)$, and then dis-

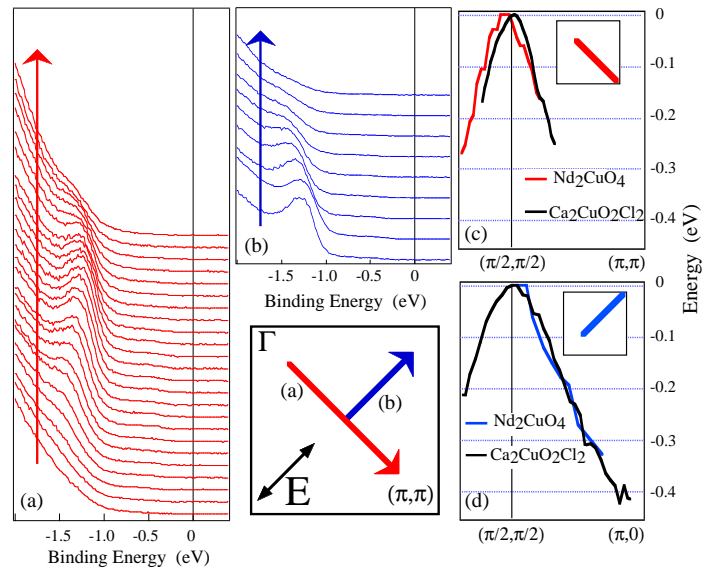


FIG. 1. (color) (a) Dispersion of charge transfer (CT) band in Nd_2CuO_4 along zone diagonal from 25% to 75% of Γ to (π, π) distance. (b) Dispersion of CTB from $(\pi/2, \pi/2)$ to 50% of the $(\pi/2, \pi/2)$ to $(\pi, 0)$ distance (c) and (d) Comparison of the CTB dispersion in NCO (red and blue) and CCOC (black)

perses back to higher energy. A very similar dispersion can be seen in the perpendicular direction (Fig. 1(b)). A dispersion with a strikingly similar shape and energy scale has been seen in SCOC and CCOC, as shown in Figs. 1(d) and 1(e). Due to this similarity, as well the fact that the feature's position relative to the chemical potential (~ 1.3 eV; minimum binding energy of its centroid) is approximately the same as this material's optical gap ~ 1.6 eV (measured from the peak position of the conductivity) [16] we assign this feature to the CTB. This assertion is supported below by its dramatic doping dependence. There is some variability (± 0.1 eV) in the exact binding energy of the CTB from cleave to cleave, as also observed in CCOC and SCOC. In Figs. 1(a) and 1(b) the horizontal scale is set to the average position from a number of samples. In Figs. 1(c) and 1(d) the energy is given relative to the binding energy minimum of the feature. Even the as-grown $x = 0$ sample is probably slightly doped so that the chemical potential is pinned near the conduction band minimum (UHB). Part of the discrepancy between photoemission (1.3 eV) and optics (1.6 eV) may stem from the fact that the charge transfer (CT) gap appears to be indirect, as we will show later. The CTB in NCO may not have been resolved previously due to an anomalous polarization dependence of its intensity, and because it is partially obscured by the main valence band [17].

Having identified the CTB in Nd_2CuO_4 , we can track it as the dopant concentration is increased and spectral weight appears in the near- E_F region. In Figs. 2(a) and 2(b) we plot partially angle-integrated energy distri-

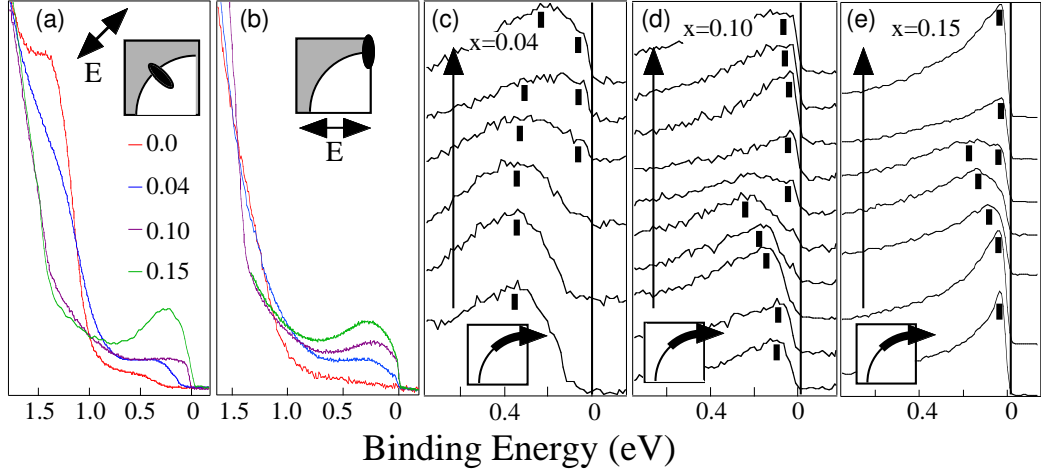


FIG. 2. (a) EDCs integrated in a region near the $(\pi/2, \pi/2)$ position. (b) EDCs integrated in a region near the $(\pi, 0.3\pi)$ position (c), (d), and (e) EDCs from around the putative LDA Fermi surface for $x = 0.04, 0.10$, and 0.15 samples, respectively

bution curves (EDCs) from regions near $(\pi/2, \pi/2)$ and $(\pi, 0.3\pi)$ respectively. In Fig. 2(a), one can see that at finite doping levels the CTB spectral weight decreases and intensity develops at energies near E_F at what is ostensibly the edge of the upper Hubbard band. This is suggestive of the kind of transfer of spectral weight from high energies to low energies that one qualitatively expects when doping a Mott insulator [6]. We make this assignment of near- E_F weight at least partially to the UHB from a comparison of its distance from the CTB to that of the optical gap energy. The CTB is not well resolved near $(\pi, 0.3\pi)$, irrespective of its intrinsic intensity, as it has dispersed back near the main valence band onset and has a strong matrix element suppression, as mentioned above.

A closer look at Fig. 2(a) reveals that there is a very weak low-energy “foot” in the $x = 0$ sample that probably reflects a small intrinsic doping level in this otherwise half-filled material. Moreover, the larger nondispersive near- E_F spectral weight that develops along the zone diagonal for the $x = 0.04$ sample is gapped by ~ 150 meV. This is in contrast to near $(\pi, 0.3\pi)$ (Fig. 2(b)), where there is spectral weight at E_F for $x = 0.04$ doping levels. For $x = 0.10$, the zone diagonal spectral weight has moved closer to E_F and even stronger E_F intensity has formed near $(\pi, 0.3\pi)$. A weak dispersion is evident along the zone diagonal for the $x = 0.10$ sample (not shown). At $x = 0.15$ there is large near- E_F weight and a strong dispersion throughout the zone as detailed in our previous work [13,14].

Following our previous analysis of the optimally doped compound [13], we construct Fermi surfaces by integrating EDCs in a small window about E_F (-40meV, +20meV) and plotting this quantity as a function of \vec{k} (Fig. 3). Consistent with the above observation that spectral weight along the zone diagonal is gapped for

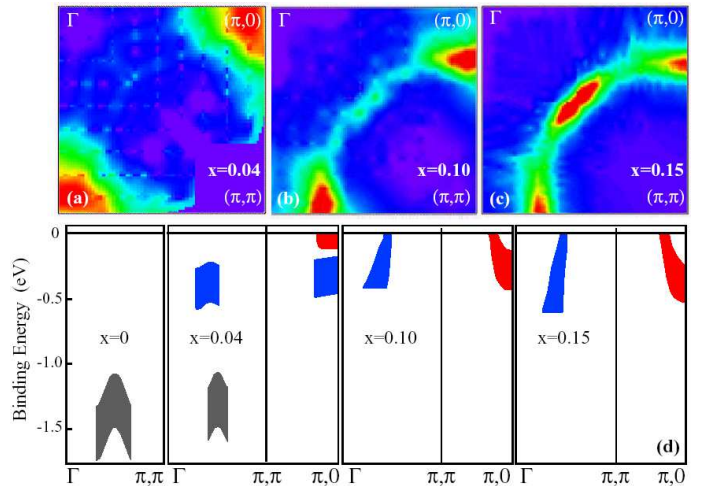


FIG. 3. (color) Fermi surface plot: (a) $x = 0.04$, (b) $x = 0.10$, and (c) $x = 0.15$. EDCs integrated in a 60meV window (-40meV, +20meV) plotted as a function of \vec{k} . Data were typically taken in the displayed upper octant and symmetrized across the zone diagonal. (d) Panels showing doping dependent “band structure”. Features are plotted for the doping levels and momentum space regions where they can be resolved. We do not include the slight low-energy shoulder of the $x = 0$ sample, as this is probably reflective of a small intrinsic doping level.

$x = 0.04$, one can see that it is only the states at $(\pi, 0)$ that can contribute to low-energy properties. Here, a Fermi “patch” indicates that there is an extremely low-energy shallow band in this part of the Brillouin zone. At $x = 0.10$, weight at E_F with low intensity begins to appear near the zone diagonal. Near $(\pi, 0)$ the “band” becomes deeper and the Fermi patch becomes a Fermi surface. At $x = 0.15$ the zone diagonal region has become intense. The full Fermi surface has formed and only in

the intensity-suppressed regions near $(0.65\pi, 0.3\pi)$ (and its symmetry-related points) does the underlying Fermi surface keep its anomalous properties [13].

We can gain more insight by looking at plots of the EDCs around the putative LDA Fermi surface, as shown in Figs. 2(c)-2(e). In Fig. 2(c), for $x = 0.04$, a large broad feature is gapped by ~ 150 meV near the zone-diagonal region. As one proceeds around the ostensible LDA Fermi surface, the high-energy feature loses spectral weight and may disappear while another feature pushes up at E_F . It is this second component that contacts E_F near $(\pi, 0.3\pi)$ to form the small Fermi surface for the $x = 0.04$ sample. Similar behavior is seen in the $x = 0.10$ and 0.15 plots; the lowest energy features become progressively sharper as one gets closer to and enters the metallic state. The fact that there are two components supports our conjecture that at low dopings the material can be characterized by a small FS or electron pocket around $(\pi, 0)$ (volume consistent with $x = 0.04$) with doping-induced spectral weight at higher energy elsewhere in the zone. As the carrier concentration is increased, the $(\pi, 0)$ FS deforms and a new FS segment emerges. The new segment derives from the diagonal feature progressively moving to E_F , as seen by comparing the bottom EDCs of Figs. 2(c)-2(e). These two segments connect to form the LDA-like Fermi surface with volume 1.12 ± 0.05 .

In the lower panels of Fig. 3 we present a schematic that shows the above described evolution of the E vs. \vec{k} relation along the two symmetry directions $\Gamma - (\pi, \pi)$ and $(\pi, \pi) - (\pi, 0)$ for our four doping levels. The centroid of the features are plotted for the doping levels and momentum space regions where they can be resolved.

The existence of a Fermi patch at $(\pi, 0)$ in the lightly doped $x = 0.04$ sample is consistent with $t - t' - t'' - U$ models which predict that the lowest electron-addition states for the insulator are near $(\pi, 0)$ [19]. This confirms an electron-hole asymmetry (broken by the higher order hopping terms) [19,20] as the lowest hole-addition states for the insulator are near $(\pi/2, \pi/2)$ [3,4,20] and is the first direct evidence for an indirect CT gap in the cuprates. However, the spectral weight that appears in the the CT gap is not explained within a simple LHB/UHB picture. Exact $t - t' - t'' - U$ model numerical calculations have shown evidence for intrinsic excitations to lie in the insulator's gap at low doping [19]. These calculations show the features to have only low spectral weight with the majority contribution at $(\pi, 0)$, as is observed. In addition, the detailed evolution of the electronic structure with doping, especially the \vec{k} space mapping of the low lying excitations of Fig. 3, bears clear resemblance to theoretical models that allow the effective U to decrease with doping [18]. Within these models, the CT gap closes with increasing doping and the Fermi level now cuts not only the bottom of the conduction band near $(\pi, 0)$, but also the top of the valence

band near $(\pi/2, \pi/2)$ because of the indirect gap [18].

Starting from the metallic side, an alternative approach may be one that emphasizes a coupling of electrons to magnetic fluctuations with characteristic wavevector (π, π) . Within this picture, as the antiferromagnetic phase is approached and antiferromagnetic correlations become stronger the "hot spot" regions (intersection of the FS and antiferromagnetic Brillouin zone boundary [13]) spread so that the zone-diagonal spectral weight is gapped by the approximate nesting of the $(\pi/2, \pi/2)$ section of FS with the $(-\pi/2, -\pi/2)$ section of FS. This scheme obviously breaks down as one gets close to the Mott state.

Our finding of an electron pocket that evolves with doping into a large hole-like Fermi surface provides a route towards explaining the long-standing puzzle that while these materials exhibit unambiguous n-type carrier behavior at low doping, one has to invoke both electron and hole-carriers to explain data near optimal doping [21].

In conclusion, it appears that certain elements of both scenarios laid out in the introduction can explain our data. At low carrier concentrations electrons are doped into regions close to $(\pi, 0)$ (confirming a particle-hole asymmetry) near the energy expected for the UHB and form a small Fermi surface. Simultaneously, there is an appearance of spectral weight at higher energy that begins to span and fill the insulator's gap. At higher electron doping levels, more spectral weight is created in this midgap region and it is this high-energy spectral weight that moves to the chemical potential and completes the \vec{k}_F segment to form a large Fermi surface with a volume close to the expected Luttinger volume.

The authors would like to thank T. Tohyama, P.G. Steeneken, C. Kusko, and B. Markiewicz for valuable correspondences. Experimental data was recorded at SSRL which is operated by the DOE Office of Basic Energy Science, Div. of Chem. Sciences and Mat. Sciences. Additional support comes from the Office of Naval Research: ONR Grants N00014-95-1-0760/N00014-98-1-0195. The crystal growth work at Tokyo was supported in part by Grant-in-Aids for Scientific Research from the Ministry of Education, Science, Sports, and Culture, Japan, and NEDO. The Stanford crystal growth was supported by the U.S. Department of Energy under contracts No. DE-FG03-99ER45773 and No. DE-AC03-76SF00515, by NSF CAREER Award No. DMR-9985067, and by the A.P. Sloan Foundation.

^a Present Address: Dept. of Physics and Astronomy, UCLA, Los Angeles, CA

^b Present Address: Dept. of Physics, University of Toronto, Toronto, Canada

^c Present Address: Dept. of Physics, Yonsei University, Seoul, Korea

^d Present Address: Dept. of Physics and Astronomy, University of British Columbia, Vancouver, Canada

- [1] P.W. Anderson and R. Schrieffer, Physics Today **44**, no. 6, 54-61 (1991).
- [2] J. Zaanen, G.A. Sawatzky, and J.W. Allen, Phys. Rev. Lett. **55**, 418 (1985).
- [3] B.O. Wells *et. al.*, Phys. Rev. Lett. **74**, 964 (1995).
- [4] F. Ronning *et al.*, Science **282**, 2067 (1998).
- [5] O. Gunnarsson, O. Jepsen, Z.-X. Shen., Phys. Rev. B. **42**, 8707 (1990).
- [6] M. Meinders, H. Eskes, G.A. Sawatzky, Phys. Rev. B **48**, 3916 (1993).
- [7] J.W. Allen *et. al.*, Phys. Rev. Lett. **64**, 595 (1990).
- [8] A. Ino *et. al.*, Phys. Rev. B **62**, 4137 (2000).
- [9] M.A. van Veenendaal and G.A. Sawatzky, Phys. Rev. B. **49**, 1407 (1994).
- [10] Z.-X. Shen and D. Dussau, Phys. Reports **253** (1995).
- [11] A. Damascelli *et. al.*, submitted Rev. Mod. Phys.
- [12] D. King *et. al.*, Phys. Rev. Lett. **70**, 3159-3162 (1993); R.O. Anderson *et. al.*, Phys. Rev. Lett. **70**, 3163-3166 (1993); T. Sato, T. Kamiyama, T. Takahashi, K. Kurahashi, and K. Yamada, Science **291**, 1517-19 (2001).
- [13] N.P. Armitage *et. al.*, Phys. Rev. Lett. **87**, 147003 (2001).
- [14] N.P. Armitage *et. al.*, Phys. Rev. Lett. **86**, 1126 (2001).
- [15] Y. Onose *et. al.*, Phys. Rev. Lett. **82**, 5120 (1999).
- [16] T. Arima *et. al.*, Phys. Rev. B. **44**, 917 (1991).
- [17] N. P. Armitage *et. al.*, *in preparation*.
- [18] C. Kusko, M. Lindroos, A. Bansil, and R.S. Markiewicz, submitted Phys. Rev. Lett.
- [19] T. Tohyama and S. Maekawa, cond-mat/0106311, submitted Phys. Rev. Lett.
- [20] C. Kim *et. al.*, Phys. Rev. Lett. **80**, 4245 (1999).
- [21] Z. Wang, *et. al.* Phys. Rev. B **43**, 3020-3025 (1991); S. Kubo, and M. Suzuki, Physica C **185-189**, 1251-1252 (1991); W. Jiang, *et. al.*, Phys. Rev. Lett. **73**, 1291-1293 (1994).